Am J Physiol Gastrointest Liver Physiol 310: G696–G704, 2016.
First published March 3, 2016; doi:10.1152/ajpgi.00443.2015.

CALL FOR PAPERS | *Physiology and GI Cancer*

Distinct miRNA profiles in normal and gastric cancer myofibroblasts and significance in Wnt signaling

Liyi Wang,[1] Islay Steele,[1] Jothi Dinesh Kumar,[1] Rod Dimaline,[1] Puthen V. Jithesh,[2] Laszlo Tiszlavicz,[3] Zita Reisz,[3] Graham J. Dockray,[1] and Andrea Varro[1]

[1]*Departments of Cellular and Molecular Physiology and* [2]*Molecular and Clinical Cancer, Institute of Translational Medicine, University of Liverpool, Liverpool, United Kingdom; and* [3]*Department of Pathology, University of Szeged, Szeged, Hungary*

Submitted 15 December 2015; accepted in final form 25 February 2016

Wang L, Steele I, Kumar JD, Dimaline R, Jithesh PV, Tiszlavicz L, Reisz Z, Dockray GJ, Varro A. Distinct miRNA profiles in normal and gastric cancer myofibroblasts and significance in Wnt signaling. *Am J Physiol Gastrointest Liver Physiol* 310: G696–G704, 2016. First published March 3, 2016; doi:10.1152/ajpgi.00443.2015.—Stromal cells influence epithelial function in both health and disease. Myofibroblasts are abundant stromal cells that influence the cellular microenvironment by release of extracellular matrix (ECM) proteins, growth factors, proteases, cytokines, and chemokines. Cancer-associated myofibroblasts (CAMs) differ from adjacent tissue (ATMs) and normal tissue myofibroblasts (NTMs), but the basis of this is incompletely understood. We report now the differential expression of miRNAs in gastric cancer CAMs. MicroRNA arrays identified differences in the miRNA profile in gastric and esophageal NTMs and in CAMs from stomach compared with NTMs. miR-181d was upregulated in gastric CAMs. Analysis of differentially regulated miRNAs indicated an involvement in Wnt signaling. Examination of a microarray data set then identified Wnt5a as the only consistently upregulated Wnt ligand in gastric CAMs. Wnt5a stimulated miR-181d expression, and knockdown of miR-181d inhibited Wnt5a stimulation of CAM proliferation and migration. Analysis of miR-181d targets suggested a role in chemotaxis. Conditioned medium from CAMs stimulated gastric cancer cell (AGS) migration more than that from ATMs, and miR-181d knockdown reduced the effect of CAM-CM on AGS cell migration but had no effect on AGS cell responses to ATM conditioned media. The data suggest that dysregulation of miRNA expression in gastric CAMs, secondary to Wnt5a signaling, accounts at least in part for the effect of CAMs in promoting cancer cell migration.

cancer; stomach; esophagus; myofibroblast; miR-181d; Wnt5a

STROMAL CELLS HAVE EMERGED IN RECENT YEARS as important determinants of epithelial cell function in the gastrointestinal mucosa in health and disease (7, 23, 25). There are multiple stromal cell types, including inflammatory and immune cells, fibroblasts, pericytes, and myofibroblasts. The latter are sparse in many tissues, but in the gut there is normally a sheath of myofibroblasts that surrounds intestinal crypts and gastric glands. They may arise from activation of fibroblasts, for example, by TGFβ, by transdifferentiation of mesenchymal stem cells (26), or by epithelial-mesenchymal transition (20). Physiologically, they play a role in wound healing. They may also influence tumor progression (26).

Myofibroblasts are often operationally defined as expressing α-smooth muscle actin (SMA), vimentin, and fibroblast activation protein and are negative for cytokeratin and usually desmin (7). An emerging body of evidence from multiple experimental platforms supports the idea that there are marked differences between different myofibroblast populations in both health and disease. For example, microarray studies reveal differences between myofibroblasts from different regions of the normal gastrointestinal tract (12). Moreover, there are marked differences in cancer at the levels of transcripts, proteins, and functions. Previously, we showed that myofibroblasts from gastric or esophageal cancer differ from their counterparts in adjacent tissue with evidence that myofibroblasts from advanced gastric tumors promote more aggressive phenotypes in cancer cells (3, 13, 14, 17). We also showed that esophageal cancer-associated myofibroblasts (CAMs) exhibit increased secretion of the chemokine-like peptide chemerin, which plays a role in mesenchymal stem cell recruitment (17).

MicroRNAs (miRNAs) are short RNAs of ~22 nucleotides that act posttranscriptionally to determine mRNA stability and translation (1). They regulate an impressive diversity of biological processes and importantly may contribute to cancer initiation and progression. In stomach and esophagus, previous studies have identified differentially expressed miRNAs (8, 11, 19). However, it is not known whether miRNAs contribute to the differences in function of different myofibroblast populations.

In view of differences in the secretomes and proteomes of gastric or esophageal cancer-derived myofibroblasts compared with their respective adjacent tissue myofibroblasts (ATMs), in the present study we sought to determine whether there might also be differences in their miRNA expression profiles compared both with each other and with normal tissue myofibroblasts (NTMs). We now report that gastric and esophageal NTM miRNA profiles are readily distinguishable, that gastric CAMs differ from their respective NTMs in their miRNA profiles, and that Wnt5a (which is upregulated in gastric CAMs) may act in part via miR-181d to influence mesenchymal-epithelial signaling.

MATERIALS AND METHODS

Cells. Human primary CAMs and ATMs had previously been generated from patients undergoing surgery for gastric or esophageal cancer. Normal myofibroblasts from both parts (antrum and corpus) of

Address for reprint requests and other correspondence: A. Varro, Dept. of Molecular & Cellular Physiology, Inst. of Translational Medicine, Univ. of Liverpool, Crown St., Liverpool L69 3BX, UK (e-mail: avarro@liv.ac.uk).

healthy stomach and esophagus had been generated from deceased transplant donors. The patients and the myofibroblasts obtained from them have been reported previously (6, 14). This work was approved by the Ethics Committee of the University of Szeged, Szeged, Hungary. Myofibroblasts were cultured as described previously and were used between passages 3 and 10 (14). AGS cells were obtained from American Type Culture Collection (Manassas, VA).

miRNA array profiling. Myofibroblasts (1.5×10^6) were cultured overnight in 7.5-cm dishes, and total RNA was extracted using miRNeasy according to the manufacturer's instructions (Qiagen, Crawley, UK). Samples were stored at −80°C. Total RNA and reference samples were labeled with Hy3™ and Hy5™ fluorescence labels, respectively (Exicon Services, Vedbaek, Denmark). The Hy3™-labeled samples and Hy5™-labeled reference RNA samples were mixed pairwise and hybridized to the miRCURY™ LNA Array version 5 that contains capture probes targeting all miRNAs for human, mouse, or rat registered in the miRBase version 14.0 (www.mirbase.org). After hybridization, microarrays were scanned using an Agilent G2565BA Microarray Scanner System (Agilent Technologies, Santa Clara, CA), and image analysis was carried out using ImaGene 8.0 software (BioDiscovery, Hawthorne, CA). Signals were background corrected (i.e., Normexp with offset value 10) and normalized using the globally weighted scatterplot smoothing (LOWESS) regression algorithm. The data set (GSE76221) is available at http://www.ncbi.nlm.nih.gov/geo/query/acc.cgi?acc=GSE76221.

Data analysis. Log_2 transformed median Hy3/Hy5 ratios were calculated using median signals on capture probe replicates and the average $\log_2$ median ratios across samples taken. The difference in $\log_2$ median ratio (ΔLMR) between sample groups was calculated and subjected to Student's *t*-test (2-tailed) or ANOVA using Bonferroni correction. The miRNA data resource was accessed at www.mirbase.org. Principal component analysis (PCA) and hierarchical clustering were performed using DNA Chip Analyzer (dChip0 software, www.dchip.org). Validated target miRNAs were obtained from the TarBase (31), miRecords (33), and MetaCore databases (GeneGo, St. Joseph, MI). Network enrichment analysis

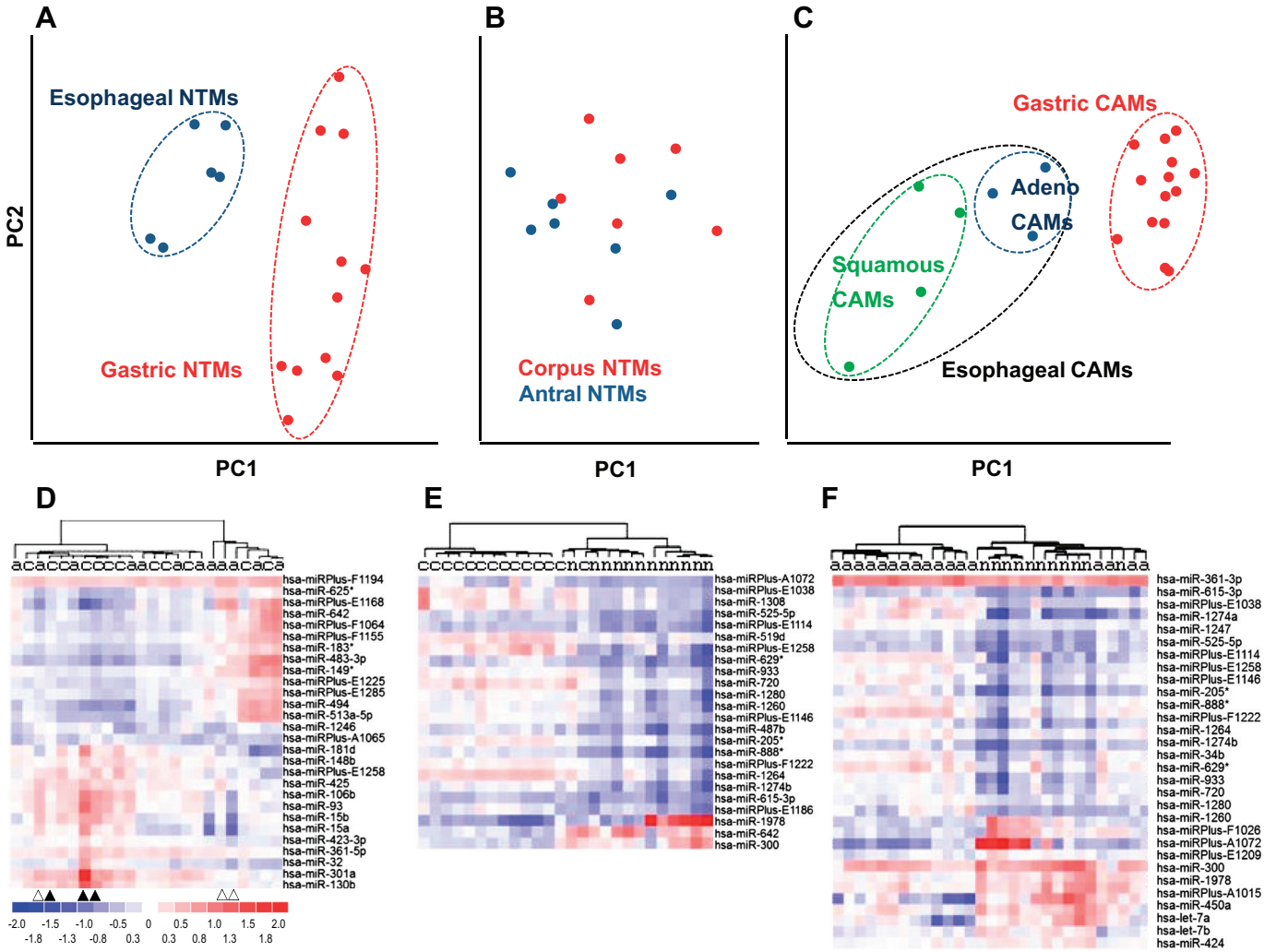

Fig. 1. Principal component analysis (PCA) and cluster analysis of miRNA expression in gastric and esophageal myofibroblasts from normal tissue and cancer. *A*: PCA of miRNA expression distinguishes myofibroblasts from normal gastric and oesophageal tissues (NTMs). *B*: PCA of miRNA expression does not distinguish antral and corpus myofibroblasts from normal stomach. *C*: PCA of miRNA expression distinguishes myofibroblasts from gastric and oesophageal cancers (CAMs); the latter includes both squamous esophageal cancer and adenocarcinoma (adeno). *D*: supervised hierarchical cluster analysis of miRNA exhibiting differential expression in myofibroblasts from CAMs (c) and ATMs (a) with a dendrogram generated by dCHip above the heat map, and scale of intensities below. To the right of the heat map are the miRNAs that are differentially expressed. The CAMs (▲) and ATMs (△) used for studies of miR-181d are indicated. *E*: supervised hierarchical clustering of miRNAs exhibiting differential expression in CAMs (c) and NTMs (n). *F*: supervised hierarchical clustering of miRNAs exhibiting differential expression in ATMs (a) and NTMs (n).

of miRNA targets was performed using MetaCore, and statistically significant networks and pathways were identified at $P < 0.05$ (FDR corrected). Predicted targets of miR-181d were retrieved from TargetScan release 5.1 (9) using a context score below −0.2 for high-efficacy targets. Gene expression profiles of gastric myofibroblasts, previously carried out using GeneChip Human Genome U133 Plus 2.0 array and deposited at http://www.ncbi.nlm.nih.gov/geo/query/acc.cgi?acc=GSE44740, (3) were used to determine the abundance of potential miRNA regulators and target transcripts.

MicroRNA quantitative PCR. MicroRNA reverse-transcription polymerase chain reaction [quantitative PCR (qPCR)] analysis was used to validate the miRNA array data. Thus, 50 ng of total RNA was reverse transcribed in 10-μl reactions using miRCURY LNA Universal RT microRNA PCR, polyadenylation, and cDNA synthesis reagents (Exicon) in triplicate. cDNA was diluted 100 times, and 4 μl was used in 10-μl PCR reactions according to the protocol for miRCURY LNA Universal RT microRNA PCR. Each miRNA was assayed once by RT-PCR. The amplification was performed in a LightCycler 480 Real-Time PCR System (Roche, Basel, Switzerland) in 384-well plates. MicroRNA qPCR analysis was also carried out using the Ambion mirVana miRNA isolation reagents (Thermo Fisher Scientific, Waltham, MA) and a 7500 real-time PCR system (Applied Biosystems, Warrington, UK) with All-in-One miRNA qRT-PCR (GeneCopoeia, Rockville, MD) according to the manufacturer's protocol in triplicate. Sequences for miRNA primers were as follows: miR-181d, 5′-AAC AUU CAU UGU UGU CGG UGG GU; miR-29b, 5′-UAG CAC CAU UUG AAA UCA GUG UU; miR-214, 5′-ACA GCA GGC ACA GAC AGG CAG U; miR-424, 5′-CAG CAG CAA UUC AUG UUU UGA A; and miR-125a-5p, 5′-UCC CUG AGA CCC UUU AAC CUG UGA.

LightCycler 480 software was used to determine the Cp value and to generate amplification and melting curves. LinRegPCR (11.5) software was used to determine the amplification efficiency. The average amplification efficiency was used to correct raw Cp values. Reference (or housekeeping) miRNAs for comparison were sought using the SLqPCR algorithm (www.bioconductor.org), which identified miR-125a-5p, miR-24, and miR-22 as appropriate stable reference miRNAs. The geometric means of these were then used to normalize measurements on a well-to-well basis. In some experiments, SDS version 1.4 software was used to determine the C_T value and product melting curves for assays of miR-181d, which were normalized to miR-125a-5p abundance in the same sample. Relative miRNA abundance was expressed using the $2^{-\Delta\Delta C_T}$ method (22).

qPCR analysis. cDNAs were prepared by reverse transcribing RNA (2 μg) with AMV reverse transcriptase (Promega, Southampton, UK) and oligoDT (Promega). Real-time PCR was carried out in an ABI 7500 thermocycler (Applied Biosystems) using Precision 2× real-time PCR master mix (Primer Design, Southampton, UK) and 5′-FAM, 3′-TAMRA double-dye probes (Eurogentec, Southampton, UK). Primers used for PCR analyses were as follows: hGAPDH probe, CGT CGC CAG CCG AGC CAC A; hGAPDH forward, GCT CCT CCT GTT CGA CAG TCA; hGAPDH reverse, ACC TTC CCC ATG GTG TCT GA; hWnt5a probe, TTT CTT TTC TGC CTC ACC CCT TTG TCT CCA; hWnt5A forward, GAA ATG CGT GTT GGG TTG AAG; and hWnt5a reverse, AAG TAA TGC CCT CTC CAC AAA G. Standard curves were generated using serial dilutions of cDNA template corresponding to the relevant gene amplicon ligated into pGEM-T Easy (Promega).

Western blot analysis. Cellular protein was extracted using RIPA lysis buffer containing 1% vol/vol Phosphatase Inhibitor Cocktail set II and 1% vol/vol Protease Inhibitor Cocktail Set III, EDTA-Free (Merk Millipore, Darmstadt, Germany). Total protein was determined using DC Protein Assay (Bio-Rad Laboratories, Hemel Hempstead, UK). Proteins were resolved by SDS-PAGE electrophoresis, transferred to nitrocellulose (Amersham Pharmacia Biotech, Buckinghamshire, UK), and incubated with antibodies to Wnt5A (R & D Systems,

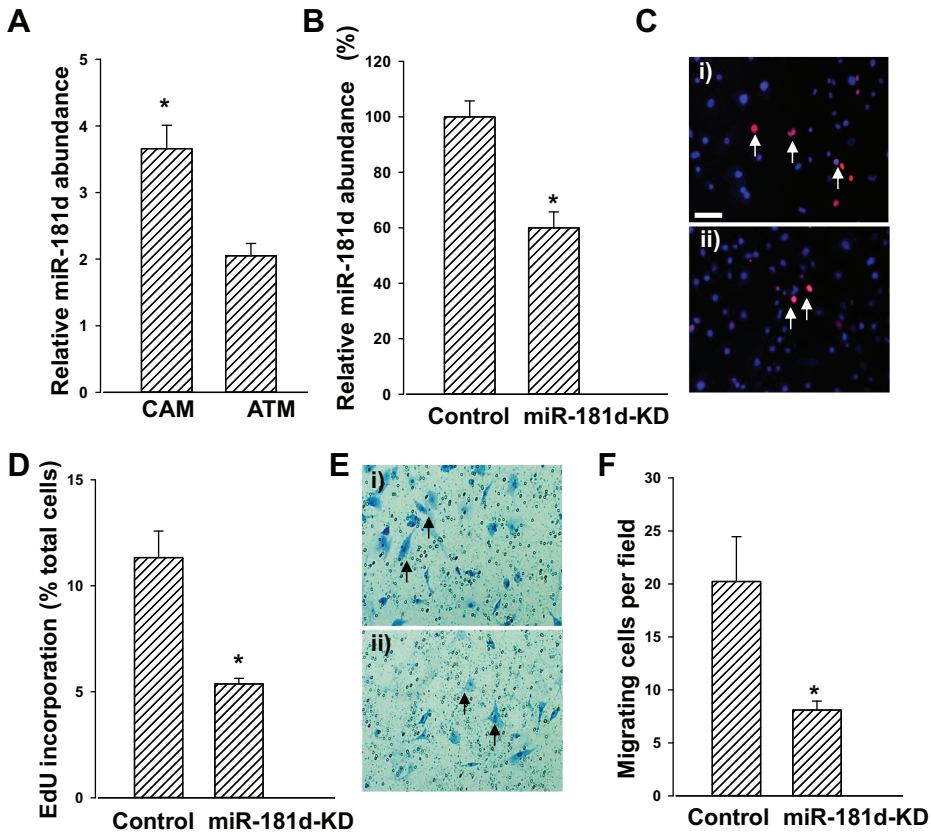

Fig. 2. Functional significance of increased miR-181d expression. *A*: increased miR-181d expression relative to miR-125a-5p in pairs of gastric CAMs and their respective ATMs; $n = 4$, $P < 0.05$. *B*: decreased relative abundance of miR-181d after miR-181d knockdown compared with control CAMs transfected with a scrambled sequence. *C*: representative images of 5-ethynyl-2′-deoxyuridine (EdU)-labeled cells (arrows) in control samples transfected with a scrambled sequence (*i*) and after mir-181d knockdown (*ii*); nuclei stained with DAPI. Scale bar, 50 μm. *D*: decreased EdU incorporation in CAMs following miR-181d knockdown (miR-181d-KD) compared with myofibroblasts transfected with scrambled controls; $n = 3$ independent experiments, $P < 0.05$. *E*: representative images of Boyden chamber experiments showing migrating control cells (arrows; *i*) and after miR-181-d knockdown (*ii*). *F*: decreased migration of CAMs after miR-181d knockdown compared with CAMs transfected with scrambled controls; $n = 3$, $P < 0.05$.

Abingdon, UK), followed by horseradish peroxidase (HRP)-conjugated secondary antibody and detection by incubation with Super-Signa West Pico Chemiluminescent Substrate (Pierce) and exposure to HyperFilm (Amersham Pharmacia Biotech). Samples of cell extracts were reprobed for GAPDH (Biodesign, Saco, Maine, USA) to normalise for protein loading. Densitometric analysis of the band intensities from Western blot analysis was performed using ImageLab software v2.1 (Bio-Rad).

Immunohistochemistry. Samples of the gastric cancers that had been used to generate myofibroblasts were fixed in 10% neutral-buffered formalin, paraffin-embedded, and processed for immunohistochemical detection of Wnt5a using mouse monoclonal antibody to Wnt5a (R & D Systems) and En Vision FLEX/HRP (Dako, Carpinteria, CA) as secondary antibody. Antigen retrieval was performed by incubating at pH 9.0, 93°C, for 15 min, as described previously (30).

miR-181d knockdown. Knockdown of miR-181d was carried out using the miArrest miRNA inhibitor clone (3 μg) (GeneCopoeia) with the appropriate control vector (3 μg), using Amaxa Human Dermal Fibroblast Nucleofector reagents (Lonza, Basel, Switzerland) and a Nucleofector I device according to the manufacturer's instructions. Cells were used for further experiments 48 h posttransfection.

Magnetofection and luciferase assays. Gastric myofibroblasts (10^5 cells/well) were seeded on six-well plates and incubated overnight in supplemented DMEM. Transfection solution was prepared according to the manufacturer's protocol and consisted of 1 μg of Cignal TCF/LEF Reporter (luciferase) construct (Qiagen), 6 μl of TransFast transfection reagent (Promega), and 2 μl of CombiMag (OZ Biosciences, Marseille, France). Posttransfection (24 h), myofibroblasts were lysed for the luciferase assay. Luciferase assay buffer II and Stop & Glo Reagent were prepared according to the manufacturer's (Promega) protocol. Activities of firefly luciferase and *Renilla* luciferase were measured by dual luciferase assay, using a Lumat LB 9507 tube luminometer (Berthold Technologies, Bad Wildbad, Germany) in triplicate. Data were presented as a ratio of firefly luciferase to *Renilla* luciferase values.

5-Ethynyl-2′-deoxyuridine incorporation. Gastric myofibroblasts (10^4/well) were seeded and incubated overnight in culture media, followed by serum starvation for 24 h. Proliferation was assessed by incorporation of 5-ethynyl-2′-deoxyuridine (EdU; 10 μM) and processing of samples using Click-iT (Invitrogen, Paisley, UK). Each experiment was performed in triplicate. EdU-positive cells were visualised on a Zeiss AxioCam HRM fluorescence microscope (Carl Zeiss, Welwyn Garden City, UK) on a ×40 objective lens, counting the total number of cell nuclei in 10 different fields using DAPI (blue; Vector Laboratories, Peterborough, UK) and EdU positive nuclei using FITC (green).

Boyden chamber migration assays. The migration of gastric myofibroblasts and AGS cells was studied using 8-μm pore Biocoat control inserts on 24 well-plates (BD Biosciences, Oxford, UK). Cell suspensions were diluted in serum-free DMEM and added to the upper chamber containing 10^4 cells. Conditioned medium (CM) or serum-free DMEM containing 1 μg/ml recombinant Wnt5a was added to each of the bottom chambers. Cells were incubated for 16 h, and migrated cells were stained on the lower surface of the membranes using the Reastain Quick-Diff kit (Reagena, Takojantie, Finland). Membranes were removed and placed on microscope slides with immersion oil (Sigma-Aldrich, Darmstadt, Germany) underneath and covered with cover slips. Cells were visualized and counted from five different fields using a ×10 objective lens and a Zeiss Axiovert25 Microscope. Each experiment was performed in triplicate.

Statistics. Results are expressed as means ± SE unless stated otherwise. Student's *t*-test was used to determine statistical significance of results and considered significant at $P < 0.05$ unless stated otherwise.

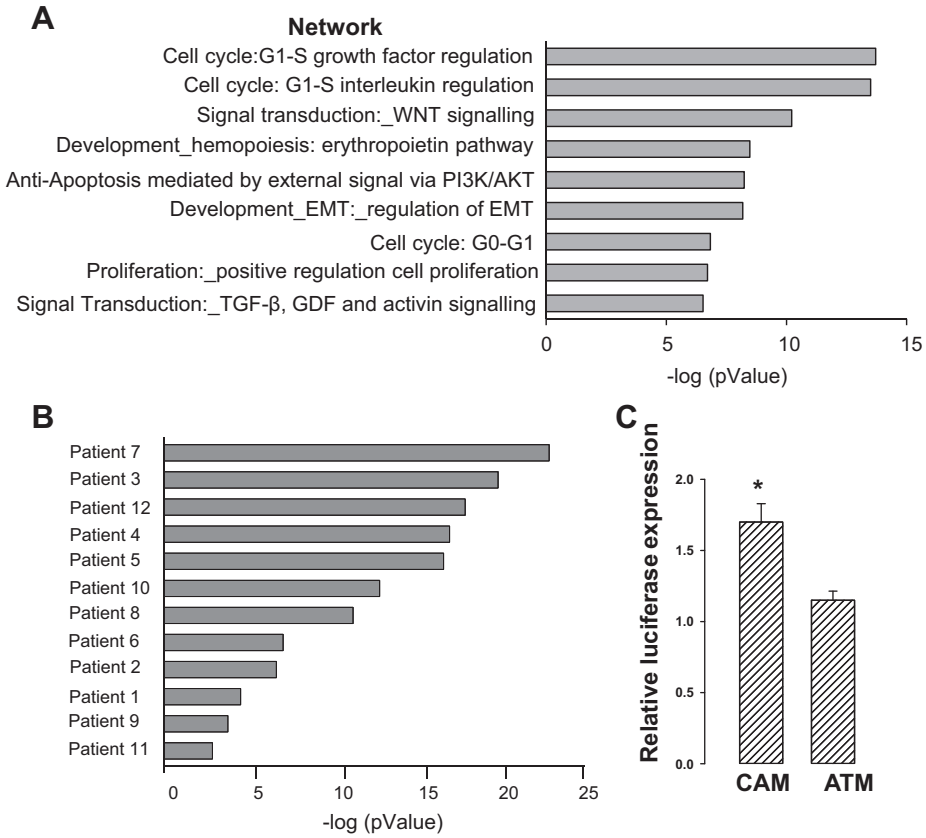

Fig. 3. MetaCore analysis of differently expressed miRNA targets in CAMs identifies a role in Wnt signaling. *A*: networks defined by enrichment of targets of the 10 miRNAs exhibiting significant differential abundance in a group of 12 CAMs compared with their respective adjacent tissue myofibroblasts (ATMs). *B*: Wnt signaling was the only network that exhibited significant enrichment [*x*-axis, −log (*P* value)] of targets of miRNAs identified as differentially expressed when each of the 12 CAMs was compared individually with their respective ATMs. *C*: increased TCF/LEF firefly luciferase activity normalized to *Renilla* luciferase in CAMs compared with ATMs; $n = 3$, $P < 0.05$. PI3K, phosphatidylinositol 3-kinase; TGFβ, transforming growth factor-β.

RESULTS

Distinct global miRNA expression profiles in normal gastric and esophageal myofibroblasts. An average of 25 and 27% of the microarray probes was detected in gastric NTMs and esophageal NTMs, corresponding to 276 and 300 mature human miRNAs, respectively. Comparison of the global miRNA data by PCA revealed distinct clusters of gastric NTMs and esophageal NTMs (Fig. 1*A*). Interestingly, normal antral- and corpus-derived myofibroblasts clustered together (Fig. 1*B*).

Different miRNA expression profiles in myofibroblasts from cancer and control tissue. The same methodology was then extended to the analysis of myofibroblasts from cancer. There were clear differences between gastric and esophageal CAMs in PCA (Fig. 1*C*). Supervised hierarchical clustering of differentially expressed miRNAs (see MATERIALS AND METHODS) did not segregate gastric CAMs vs. ATMs (Fig. 1*D*); however, there was segregation of gastric CAMs from NTMs (Fig. 1*E*) and of gastric ATMs from NTMs (Fig. 1*F*).

Validation of microarray analysis. The microarray data were initially validated by applying qPCR to gastric and esophageal myofibroblasts for three miRNAs (miR-29b, miR-214, and miR-424). These were selected on the basis that they were well expressed in both tissues, which gave a relatively large sample size for comparison. Thus, there was a positive correlation between microarray and qPCR analyses for miR-29b (Pearson correlation coefficient: 0.901, $P < 0.05$, $n = 43$), miR-214 (Pearson correlation coefficient: 0.685, $P < 0.05$, $n = 21$), and miR-424 (Pearson correlation coefficient: 0.926, $P < 0.05$, $n = 31$).

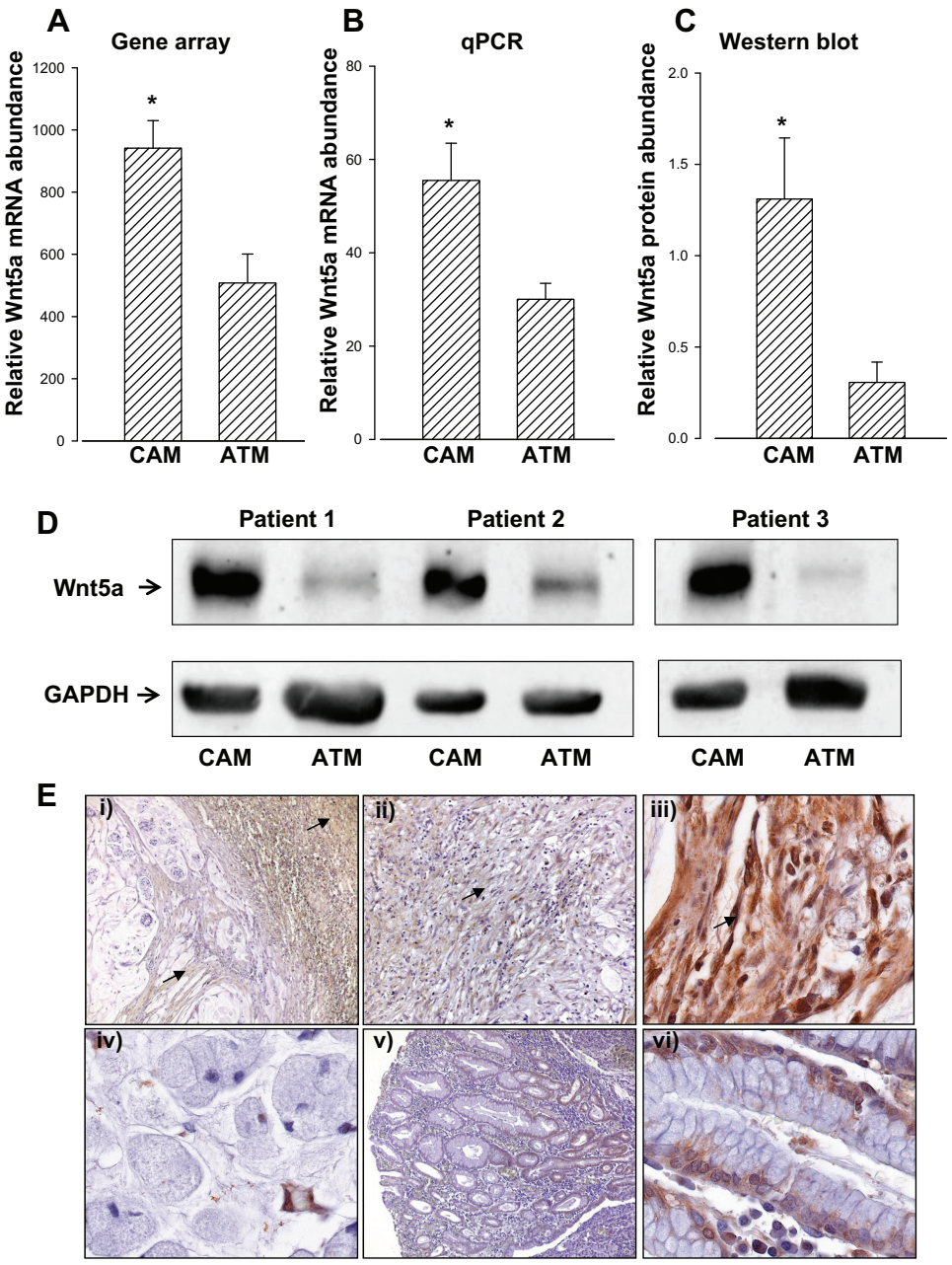

Fig. 4. Increased expression of Wnt5a in CAMs. *A:* quantification of Wnt5a mRNA abundance relative to GAPDH obtained from archived microarray data for 12 pairs of CAMs and their respective ATMs; $P < 0.05$. *B*: quantification of Wnt5a mRNA expression relative to GAPDH determined by quantitative PCR (qPCR) for pairs of CAMs and ATMs, $n = 9$; $P < 0.05$. *C*: densitometrical quantification of Wnt5a protein abundance relative to GAPDH determined by Western blot for pairs of CAMs and ATMs; $n = 6$, $P < 0.05$. *D*: representative Western blots of Wnt5a and GAPDH of CAMs and ATMs. *E*: immunohistochemical localization of Wnt5a in gastric cancer and adjacent tissues. Arrows indicate staining in stromal cells in cancer (*i*, ×10; *ii*, ×20; *iii*, ×40) compared with adjacent cancer tissue (*iv*, ×40) or control tissue (*v*, ×10; *vi*, ×40).

Of the miRNAs that exhibited significant differential abundance in gastric CAMs vs. ATMs (Fig. 1*D*), miR-181d exhibited the highest mean difference (Fig. 2*A*). For validation of miR-181d by qPCR, we selected three pairs of CAMs and ATMs, including the two that exhibited the widest difference in miR-181d expression; there was good agreement between qPCR and microarrays in miR-181d relative abundance in CAMs/ATMs (microarrays 1.7 ± 0.4, compared with 1.8 ± 0.3 by qPCR). The two pairs of CAMs and ATMs exhibiting the highest difference in expression were then used for functional validation studies. In particular, the relevance of miR-181d to the CAM phenotype was indicated by the observation that knockdown of miR-181-d (Fig. 2*B*) significantly reduced both incorporation of EdU (Fig. 2, *C* and *D*) and migration in Boyden chambers (Fig. 2, *E* and *F*).

Network analysis of differentially abundant miRNAs in CAMs vs. ATMs. There were 10 miRNAs that exhibited significant differential abundance when the data from gastric CAMs and ATMs as a whole were compared, and for which published and validated targets were available in MetaCore, TargetScan5.1, TarBase, or miRecods. The validated targets for these miRNAs were then taken for network analysis in MetaCore. The top three networks exhibiting significant enrichment were implicated in proliferation and Wnt signaling (Fig. 3*A*). To determine whether there was interpatient variability in enriched networks, we then performed a pairwise comparison of CAMs and ATMs from each of 12 patients. For this analysis, we identified miRNAs exhibiting ≥50% difference in abundance in each pair; as before, validated targets of these miRNAs were then used for network analysis in MetaCore. This analysis revealed Wnt signaling as significantly enriched in all 12 pairs; this was the only network to be significantly enriched in all cases (Fig. 3*B*). However, in addition, regulation of proliferation was enriched in 11 of 12 pairs of CAMs and ATMs.

Consistent with these findings, we have reported previously that CAMs exhibit increased proliferation, as well as increased migration and reduced apoptosis, compared with ATMs (14,

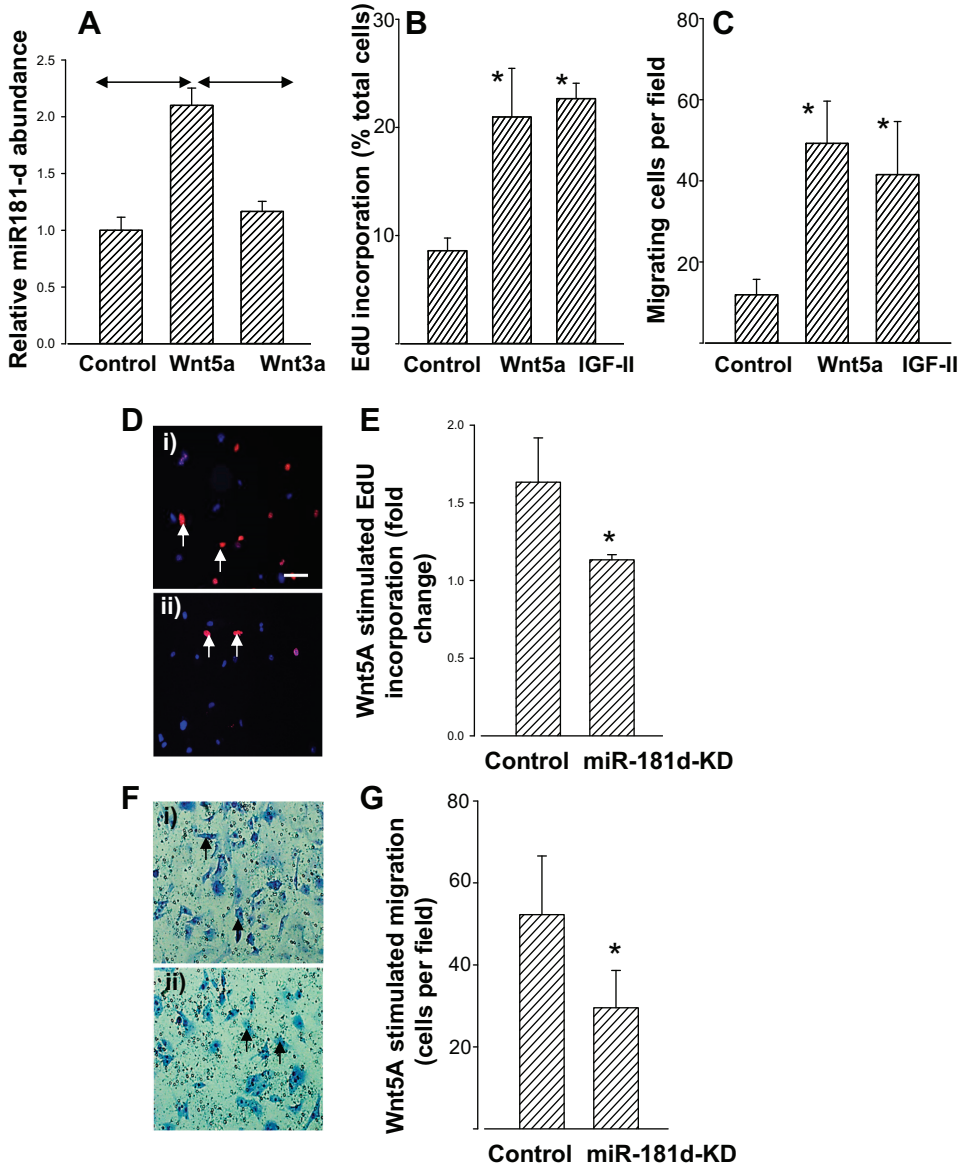

Fig. 5. Increased miR-181d expression by Wnt5a. *A*: increased miR-181d expression determined by qPCR in response to Wnt5a (1 μg/ml), but not Wnt3a (1 μg/ml), expressed relative to miR125a-5p; $n = 3$, Horizontal double arrows, $P < 0.05$, ANOVA. *B*: Wnt5a and IGF-II (100 ng/ml) have similar effects in stimulating EdU incorporation. *C*: Wnt5A and IGF-II have similar effects in stimulating migration in Boyden chambers. *D*: representative image showing EdU incorporation (arrows) in CAMs in response to Wnt5a alone (*i*) and Wnt5a after knockdown of miR-181d (*ii*); nuclei stained with DAPI. Scale bar, 50 μm. *E*: EdU incorporation in CAMs in response to Wnt5a is significantly reduced by miR-181d knockdown; $n = 3$, $P < 0.05$. *F*: representative images of Boyden chamber experiments showing migrating cells (arrows) in response to Wnt5a alone (*i*) and Wnt5a after miR-181-d knockdown (*ii*). *G*: Wnt5a-stimulated migration (control) is reduced after miR-181d knockdown; $n = 3$, $P < 0.05$. *$P < 0.05$.

17). However, the identification of Wnt signaling as a prominent differentially regulated network has not previously received attention and was considered sufficiently interesting to merit further investigation. To this end, we initially explored the potential activation of Wnt signaling in CAMs using a TCF/LEF reporter assay. Luciferase activity was significantly higher in CAMs than in ATMs (Fig. 3*C*), indicating that the canonical signaling pathway is activated in CAMs.

Differential Wnt5a abundance in CAMs. There is evidence that Wnt signaling regulates miR-181 family members (15). To understand the possible role of Wnt signaling in gastric CAMs, we first examined gene array data to determine the pattern of expression of Wnt ligands with a view to identifying any that exhibited differential expression in CAMs. Out of 18 Wnt ligands represented on the array, only Wnt5a and Wnt5b were detected in all 12 pairs of CAMs and ATMs. In 10 pairs, the abundance of Wnt5a was >50% greater in CAMs than in ATMs, whereas in the other two it was unchanged; overall, the increased expression in CAMs was statistically significant (Fig. 4*A*). In contrast, Wnt5b was increased in only five pairs of CAMs compared with ATMs. Wnt2b was detected in 8 pairs, and the remainder (Wnt1, -2, -3, -4, -6, -7a, -7b, -8a, -8b, -9a, -9b, -10a, -10b, -11, and -16) were identified in fewer than half of the pairs of CAMs and ATMs. The increased expression of Wnt5a in CAMs was then confirmed by qPCR (Fig. 4*B*). Moreover, when we examined Wnt5a expression by Western blot, we found increased abundance in CAMs compared with their respective ATMs (Fig. 4, *C* and *D*). In addition, immunohistochemistry identified Wnt5a in stromal cells in gastric cancer (Fig. *4E*); a similar proportion of stromal cells (~75%) showed Wnt5a expression in cancers and adjacent tissue, but there was increased staining intensity in the tumor-associated cells.

Wnt5a stimulates mir-181d expression. Because Wnt5a was increased in gastric CAMs, we then examined whether miR-181d might mediate Wnt5a actions. There was a significant increase in miR-181d abundance in gastric myofibroblasts exposed to Wnt5a (1 μg/ml), but not Wnt3a (1 μg/ml), used for comparison (Fig. 5*A*). When CAMs were treated with Wnt5a, there was stimulation of EdU incorporation that was comparable to that seen with IGF-II (100 ng/ml) used as a positive control (Fig. 5*B*); moreover, Wnt5a stimulated migration in Boyden chambers, and the response was similar to that with IGF-II (Fig. 5*C*). After knockdown of mi-R181d, EdU incorporation in response to Wnt5a was reduced (Fig, 5, *D* and *E*). Similarly, Wnt5a-stimulated migration was significantly reduced after knockdown of mi-R181d (Fig. 5, *F* and *G*). The specificity of the response was indicated by the fact that miR-181d did not inhibit the migratory response to IGF-II (IGF-II, 61.3 ± 5.1 cells/field; IGF-II and miR-181d knockdown, 57.7 ± 3.5).

Network analysis of miR-181d targets identifies chemotactic networks. We then examined in MetaCore the published and validated targets of miR-181d; in view of the importance of myofibroblasts in determining the tumor microenvironment, we focused on targets encoding extracellular proteins. This analysis identified regulation of chemotaxis as the top enriched network (Fig. 6*A*). This was considered interesting since it is known that conditioned medium (CM) from CAMs stimulates cancer cell migration more than CM from ATMs (14). To

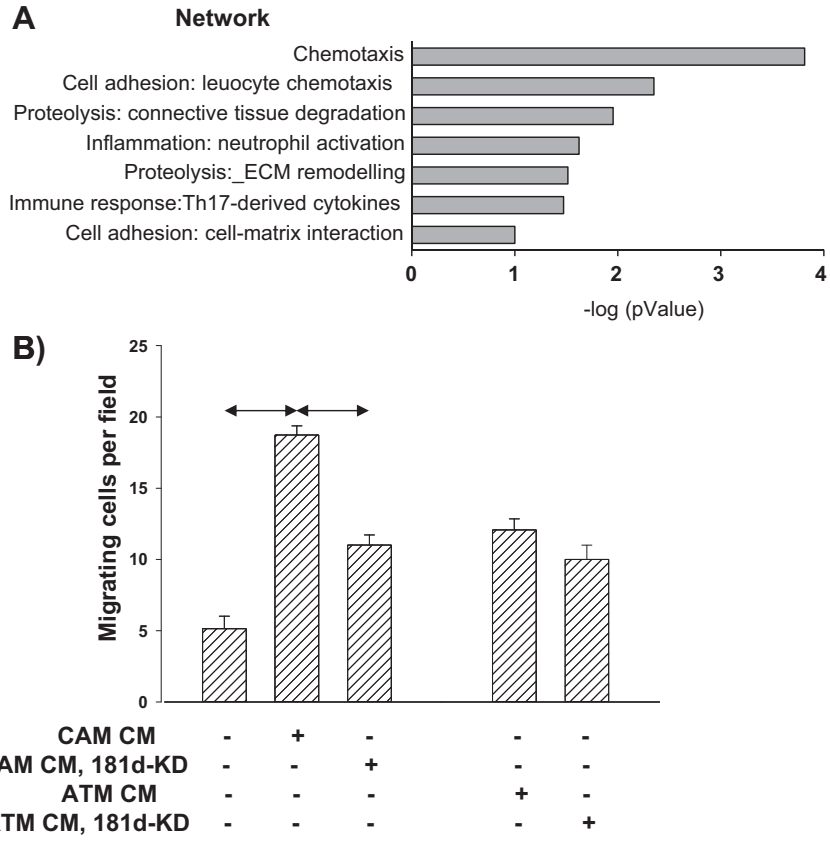

Fig. 6. MetaCore analysis of differently expressed miRNA target genes encoding secreted proteins in CAMs identifies a role in chemotaxis. *A*: networks enriched by targets encoding secreted proteins of significantly differently expressed miRNAs in CAMs compared with ATMs. *B*: conditioned media (CM) from control transfected CAMs (CAM CM) stimulates migration of gastric cancer cells (AGS) in Boyden chambers, but this is reduced after miR-181d knockdown in the CAMs (CAM CM, 181d-KD); in contrast, CM from ATMs (AMT CM) has a smaller effect on AGS cell migration, and pretreatment of the ATMs to knockdown miR-181d (ATM CM, 181d-KD) has no effect on the response; $n = 3$ horizontal arrows, $P < 0.05$, ANOVA.

determine whether miR-181d is implicated in this mechanism, gastric cancer AGS cells were incubated with CAM CM after miR-181d knockdown. CM from CAMs significantly stimulated AGS cell chemotaxis, and there was a significant decrease in migration of AGS cells in CM from miR-181d knockdown CAMs (Fig. 6*B*). In contrast, ATM CM stimulated a smaller migratory response, and knockdown of miR-181d in the ATMs had no effect (Fig. 6*B*).

DISCUSSION

The main finding of this study is that there are different miRNA profiles in myofibroblasts from normal stomach and esophagus and in gastric cancer-derived myofibroblasts compared with control tissue. We show that miR-181d is increased in gastric CAMs and mediates the actions of Wnt5a, which is itself upregulated in these cells. Medium from CAMs stimulates cancer cell migration, and this is decreased by miR-181d knockdown. The data suggest that differential regulation of miRNAs in myofibroblasts may promote an aggressive phenotype in gastric cancer cells.

There is growing appreciation of the diversity of cells of fibroblastic lineages in the gastrointestinal tract with distinct transcriptomes in cells from different regions (12) as well as in cells from cancer or adjacent tissue (14, 17). There are likely to be multiple underlying mechanisms, and, for example, it is already known that there are epigenetic differences between gastric CAMs and ATMs (16). The present data now identify variable expression of miRNAs in different myofibroblast populations. We were readily able to distinguish the miRNA profiles of gastric and esophageal myofibroblasts from normal healthy tissue as well as from gastric cancer and normal tissue. Therefore, the data emphasize the importance of selecting the appropriate myofibroblasts for studies of stromal-epithelial cell function. The physiological significance of the heterogeneity in gastrointestinal myofibroblasts remains uncertain. In the present study we focused on gastric cancer, but in the future it should be possible to perform similar studies in esophagus. The present studies identify dysregulation of miR-181d and a link to increased Wnt5a expression, both of which have previously been associated with gastric cancer (2, 18).

The relationship between miRNA profiles and Wnt signaling in myofibroblasts is complex. Both the canonical and noncanonical Wnt pathways have been linked to myofibroblast function. The canonical pathway has been implicated in differentiation of myofibroblasts from fibroblasts and mesenchymal stem cells (4, 29). Moreover, the present observations on increased activity in gastric CAMs of a TCF/LEF reporter construct are consistent with enhanced canonical pathway activation. In addition, however, it is known that the noncanonical ligand Wnt5a is expressed in gastrointestinal myofibroblasts and can be upregulated in response to stimulation, whereas a range of other Wnt family members were either absent or unchanged (21). Our evidence suggests that Wnt5a is the predominant Wnt ligand to be expressed in gastric myofibroblasts. Several lines of evidence (microarray, qPCR, Western blot, immunohistochemistry) point to increased expression of Wnt5a in CAMs compared with ATMs. We showed that Wnt5a stimulated proliferation, migration, and miR-181d expression in gastric myofibroblasts and that knockdown of miR-181d inhibited the proliferative and migratory responses to Wnt5a. Therefore, the data provide a functional framework for interpreting previous studies showing Wnt5a upregulation in gastric cancer but not gastric cancer cell lines, which was considered to suggest an association with the presence of stroma (27). Even so, the mechanism responsible for increased Wnt5a expression in gastric cancer remains unknown, and further work is required here. Nevertheless, since Wnt5a expression is linked to poor outcome (18) in gastric cancer, the identification of a downstream pathway involving miR-181d may prove useful in diagnosis and therapy. In this context, it is worth mentioning that other studies have reported the increased expression Dickkopf-1 in gastric cancer (10) and secreted frizzled related protein-1 (24), both of which were associated with poor outcome and both of which are potential modulators of Wnt signaling, providing further evidence of the complexity of the system.

There is increased expression of miR-181d in a number of cancers, including acute myeloid leukemia (28) and gastric cancer (2), although there is downregulation in gliomas (5). In liver, increased expression of miR-181d is associated with progression to hepatocellular carcinoma; in this setting, miR-181d is regulated by TGFβ, and one of its targets is tissue inhibitor of metalloproteinase 3 (TIMP3) (32). Our findings indicate that knockdown of miR-181d in CAMs reduced the effect of CAM-CM on AGS cell migration, pointing to miR-181d suppression of an inhibitor of migration. There is increased MMP activity in gastric CAM CM that contributes to stimulation of cancer cell migration (13) so that suppression by miR-181d of MMP inhibitors such as TIMP3 provides a mechanism for understanding how expression of miR-181d in stromal cells promotes an aggressive phenotype in gastric cancer cells.

ACKNOWLEDGMENTS

We thank Dr. Lucille Rainbow for help with miRNA preparation.

Present address of P. V. Jithesh: Sidra Medical and Research Centre, Doha, Qatar.

GRANTS

This work was supported by grants from the Wellcome Trust and North West Cancer Research.

DISCLOSURES

The authors disclose no conflicts of interest, financial or otherwise.

AUTHOR CONTRIBUTIONS

L.W., I.S., R.D., L.T., and Z.R. performed experiments; L.W., I.S., J.D.K., R.D., P.V.J., L.T., and Z.R. analyzed data; L.W. and A.V. prepared figures; L.W., I.S., J.D.K., R.D., P.V.J., L.T., Z.R., G.J.D., and A.V. approved final version of manuscript; P.V.J. interpreted results of experiments; G.J.D. and A.V. conception and design of research; G.J.D. and A.V. drafted manuscript; G.J.D. and A.V. edited and revised manuscript.

REFERENCES

1. **Ambros V.** The functions of animal microRNAs. *Nature* 431: 350–355, 2004.
2. **An J, Pan Y, Yan Z, Li W, Cui J, Yuan J, Tian L, Xing R, Lu Y.** MiR-23a in amplified 19p13.13 loci targets metallothionein 2A and promotes growth in gastric cancer cells. *J Cell Biochem* 114: 2160–2169, 2013.
3. **Balabanova S, Holmberg C, Steele I, Ebrahimi B, Rainbow L, Burdyga T, McCaig C, Tiszlavicz L, Lertkowit N, Giger OT, Oliver S, Prior I, Dimaline R, Simpson D, Beynon R, Hegyi P, Wang TC, Dockray GJ, Varro A.** The neuroendocrine phenotype of gastric myofi-

broblasts and its loss with cancer progression. *Carcinogenesis* 35: 1798–1806, 2014.
4. **Carthy JM, Garmaroudi FS, Luo Z, McManus BM.** Wnt3a induces myofibroblast differentiation by upregulating TGF-beta signaling through SMAD2 in a beta-catenin-dependent manner. *PLoS One* 6: e19809, 2011.
5. **Ciafre SA, Galardi S, Mangiola A, Ferracin M, Liu CG, Sabatino G, Negrini M, Maira G, Croce CM, Farace MG.** Extensive modulation of a set of microRNAs in primary glioblastoma. *Biochem Biophys Res Commun* 334: 1351–1358, 2005.
6. **Czepan M, Rakonczay Z Jr, Varro A, Steele I, Dimaline R, Lertkowit N, Lonovics J, Schnur A, Biczo G, Geisz A, Lazar G, Simonka Z, Venglovecz V, Wittmann T, Hegyi P.** NHE1 activity contributes to migration and is necessary for proliferation of human gastric myofibroblasts. *Pflugers Arch* 463: 459–475, 2012.
7. **De Wever O, Van Bockstal M, Mareel M, Hendrix A, Bracke M.** Carcinoma-associated fibroblasts provide operational flexibility in metastasis. *Semin Cancer Biol* 25: 33–46, 2014.
8. **Feber A, Xi L, Luketich JD, Pennathur A, Landreneau RJ, Wu M, Swanson SJ, Godfrey TE, Litle VR.** MicroRNA expression profiles of esophageal cancer. *J Thorac Cardiovasc Surg* 135: 255–260; discussion 260, 2008.
9. **Friedman RC, Farh KK, Burge CB, Bartel DP.** Most mammalian mRNAs are conserved targets of microRNAs. *Genome Res* 19: 92–105, 2009.
10. **Gao C, Xie R, Ren C, Yang X.** Dickkopf-1 expression is a novel prognostic marker for gastric cancer. *J Biomed Biotechnol* 2012: 804592, 2012.
11. **Guo J, Miao Y, Xiao B, Huan R, Jiang Z, Meng D, Wang Y.** Differential expression of microRNA species in human gastric cancer versus non-tumorous tissues. *J Gastroenterol Hepatol* 24: 652–657, 2009.
12. **Higuchi Y, Kojima M, Ishii G, Aoyagi K, Sasaki H, Ochiai A.** Gastrointestinal Fibroblasts Have Specialized, Diverse Transcriptional Phenotypes: A Comprehensive Gene Expression Analysis of Human Fibroblasts. *PLoS One* 10: e0129241, 2015.
13. **Holmberg C, Ghesquiere B, Impens F, Gevaert K, Kumar JD, Cash N, Kandola S, Hegyi P, Wang TC, Dockray GJ, Varro A.** Mapping proteolytic processing in the secretome of gastric cancer-associated myofibroblasts reveals activation of MMP-1, MMP-2, and MMP-3. *J Proteome Res* 12: 3413–3422, 2013.
14. **Holmberg C, Quante M, Steele I, Kumar J, Balabanova S, Duval C, Czepan M, Rakonczayjr Z, Tiszlavicz L, Nemeth I, Lazar G, Simonka Z, Jenkins R, Hegyi P, Wang T, Dockray G, Varro A.** Release of TGFbetaig-h3 by gastric myofibroblasts slows tumor growth and is decreased with cancer progression. *Carcinogenesis* 33: 1553–1562, 2012.
15. **Ji J, Yamashita T, Wang XW.** Wnt/beta-catenin signaling activates microRNA-181 expression in hepatocellular carcinoma. *Cell Biosci* 1: 4, 2011.
16. **Jiang L, Gonda TA, Gamble MV, Salas M, Seshan V, Tu S, Twaddell WS, Hegyi P, Lazar G, Steele I, Varro A, Wang TC, Tycko B.** Global hypomethylation of genomic DNA in cancer-associated myofibroblasts. *Cancer Res* 68: 9900–9908, 2008.
17. **Kumar JD, Holmberg C, Kandola S, Steele I, Hegyi P, Tiszlavicz L, Jenkins R, Beynon RJ, Peeney D, Giger OT, Alqahtani A, Wang TC, Charvat TT, Penfold M, Dockray GJ, Varro A.** Increased expression of chemerin in squamous esophageal cancer myofibroblasts and role in recruitment of mesenchymal stromal cells. *PLoS One* 9: e104877, 2014.
18. **Kurayoshi M, Oue N, Yamamoto H, Kishida M, Inoue A, Asahara T, Yasui W, Kikuchi A.** Expression of Wnt-5a is correlated with aggressiveness of gastric cancer by stimulating cell migration and invasion. *Cancer Res* 66: 10439–10448, 2006.
19. **Mathe EA, Nguyen GH, Bowman ED, Zhao Y, Budhu A, Schetter AJ, Braun R, Reimers M, Kumamoto K, Hughes D, Altorki NK, Casson AG, Liu CG, Wang XW, Yanaihara N, Hagiwara N, Dannenberg AJ, Miyashita M, Croce CM, Harris CC.** MicroRNA expression in squamous cell carcinoma and adenocarcinoma of the esophagus: associations with survival. *Clin Cancer Res* 15: 6192–6200, 2009.
20. **McCracken KW, Cata EM, Crawford CM, Sinagoga KL, Schumacher M, Rockich BE, Tsai YH, Mayhew CN, Spence JR, Zavros Y, Wells JM.** Modelling human development and disease in pluripotent stem-cell-derived gastric organoids. *Nature* 516: 400–404, 2014.
21. **Pacheco II, Macleod RJ.** CaSR stimulates secretion of Wnt5a from colonic myofibroblasts to stimulate CDX2 and sucrase-isomaltase using Ror2 on intestinal epithelia. *Am J Physiol Gastrointest Liver Physiol* 295: G748–G759, 2008.
22. **Pfaffl MW.** A new mathematical model for relative quantification in real-time RT-PCR. *Nucleic Acids Res* 29: e45, 2001.
23. **Powell DW, Pinchuk IV, Saada JI, Chen X, Mifflin RC.** Mesenchymal cells of the intestinal lamina propria. *Annu Rev Physiol* 73: 213–237, 2011.
24. **Qu Y, Ray PS, Li J, Cai Q, Bagaria SP, Moran C, Sim MS, Zhang J, Turner RR, Zhu Z, Cui X, Liu B.** High levels of secreted frizzled-related protein 1 correlate with poor prognosis and promote tumourigenesis in gastric cancer. *Eur J Cancer* 49: 3718–3728, 2013.
25. **Quail DF, Joyce JA.** Microenvironmental regulation of tumor progression and metastasis. *Nat Med* 19: 1423–1437, 2013.
26. **Quante M, Tu SP, Tomita H, Gonda T, Wang SS, Takashi S, Baik GH, Shibata W, Diprete B, Betz KS, Friedman R, Varro A, Tycko B, Wang TC.** Bone marrow-derived myofibroblasts contribute to the mesenchymal stem cell niche and promote tumor growth. *Cancer Cell* 19: 257–272, 2011.
27. **Saitoh T, Mine T, Katoh M.** Frequent up-regulation of WNT5A mRNA in primary gastric cancer. *Int J Mol Med* 9: 515–519, 2002.
28. **Su R, Lin HS, Zhang XH, Yin XL, Ning HM, Liu B, Zhai PF, Gong JN, Shen C, Song L, Chen J, Wang F, Zhao HL, Ma YN, Yu J, Zhang JW.** MiR-181 family: regulators of myeloid differentiation and acute myeloid leukemia as well as potential therapeutic targets. *Oncogene* 34: 3226–3239, 2015.
29. **Sun Z, Wang C, Shi C, Sun F, Xu X, Qian W, Nie S, Han X.** Activated Wnt signaling induces myofibroblast differentiation of mesenchymal stem cells, contributing to pulmonary fibrosis. *Int J Mol Med* 33: 1097–1109, 2014.
30. **Varro A, Kenny S, Hemers E, McCaig C, Przemeck S, Wang TC, Bodger K, Pritchard DM.** Increased gastric expression of MMP-7 in hypergastrinemia and significance for epithelial-mesenchymal signaling. *Am J Physiol Gastrointest Liver Physiol* 292: G1133–G1140, 2007.
31. **Vergoulis T, Vlachos IS, Alexiou P, Georgakilas G, Maragkakis M, Reczko M, Gerangelos S, Koziris N, Dalamagas T, Hatzigeorgiou AG.** TarBase 6.0: capturing the exponential growth of miRNA targets with experimental support. *Nucleic Acids Res* 40: D222–D229, 2012.
32. **Wang B, Hsu SH, Majumder S, Kutay H, Huang W, Jacob ST, Ghoshal K.** TGFbeta-mediated upregulation of hepatic miR-181b promotes hepatocarcinogenesis by targeting TIMP3. *Oncogene* 29: 1787–1797, 2010.
33. **Xiao F, Zuo Z, Cai G, Kang S, Gao X, Li T.** miRecords: an integrated resource for microRNA-target interactions. *Nucleic Acids Res* 37: D105–D110, 2009.